Conversion electron and yrast state measurements in ^{73}Br

J. Heese, N. Martin, C. J. Gross, W. Fieber, and K. P. Lieb
II. Physikalisches Institut der Universität Göttingen, D-3400 Göttingen, Federal Republic of Germany

A. Kuhnert, K. H. Maier, and X. Sun*
Hahn-Meitner Institut Berlin G.m.b.H., D-1000 Berlin 39, Federal Republic of Germany
(Received 25 October 1989)

Gamma-ray and conversion electron measurements have been performed in the reactions ^{58}Ni(^{24}Mg,2αp)^{73}Br at 110 MeV and ^{40}Ca(^{36}Ar,3p)^{73}Br at 130 MeV, respectively. From $\gamma\gamma$ coincidence data the previously known level scheme was confirmed and extended up to probable spin $I = \frac{45}{2}$. In the conversion electron spectra, the decay of the previously postulated 27 keV state was observed for the first time. From the measurement of internal conversion coefficients, multipolarities of seven transitions in the bandhead region of ^{73}Br were determined and allowed spin-parity assignments to be established. High spin properties and quasiparticle alignment effects are discussed in comparison with ^{75}Br.

I. INTRODUCTION

The neutron deficient Se, Br, and Kr isotopes display a variety of structural effects. The experimental level schemes of ^{70,72}Se reflect the coexistence of prolate and oblate deformed shapes at low spins while near-rigid rotational motion occurs after the $g_{9/2}$ proton and neutron alignments.[1-4] In contrast, the neighboring odd-Z Br isotopes ^{73,75}Br already show large prolate deformation in the 1qp bands and nearly unperturbed rotational bands.[5-8] There are many indications that the coupling of the odd proton to the shape-coexistent core stabilizes the prolate minimum in the total energy surface.

In a previous study on ^{73}Br,[7] we reported on the measurement of level energies, lifetimes, γ-ray angular distribution coefficients, and g factors. Spin and parity assignments were based on measured γ-ray angular distributions, branching ratios, and level lifetimes. However, we were not able to unambiguously fix those assignments due to the complex level structure in the bandhead region and the unknown ground state spin. The main motivation of this work was, therefore, to measure internal conversion coefficients (ICC) of transitions in the ^{73}Br bandhead region to obtain more detailed information about their multipolarities.

In addition, a study of high spin states was performed to highlight the rotational structure and band crossing effects. This part of the present work was triggered by the observation of a successive alignment of $g_{9/2}$ proton and neutron pairs in the negative-parity yrast bands in ^{75}Br,[8] leading up to (5qp) states. This required an extension of the yrast band up to 0.8–1.0 MeV rotational frequency, i.e., above the spin $\frac{33}{2}$ established in the previous experiment.[7]

II. EXPERIMENTAL TECHNIQUES AND RESULTS

A. $\gamma\gamma$ coincidence measurements

High spin states in ^{73}Br were studied with the reaction ^{58}Ni(^{24}Mg,2αp) at 110 MeV. The Mg beam was provided by the NSF tandem accelerator of the Daresbury Laboratory. A stack of two 0.5 mg/cm^2 self-supporting, rolled ^{58}Ni foils, enriched to 99.9%, was used. The thin target allowed the evaporation residues to recoil out of the target and decay in flight. The γ radiation was detected in 15 BGO-Compton suppressed Ge detectors mounted in the back angles of the ESSA 30 frame. $\gamma\gamma$ coincidence events were stored in a $2K \times 2K$ matrix from which the individual gates were projected. Further experimental details can be obtained from Ref. 9.

Figure 1 shows spectra in coincidence with known transitions in ^{73}Br. Seven new yrast transitions were found and the γ-ray energies for six known transitions above spin $\frac{23}{2}$ were measured with higher precision. In this manner, the high spin transitions in ^{73}Br, ^{75}Br,[8] ^{78}Sr,[9] and ^{76,78}Kr,[10] which were all produced in the ^{58}Ni+^{24}Mg reaction, now are based on a common energy calibration. The proposed new level scheme of ^{73}Br is shown in Fig. 2. No band based on the 27 keV state has been observed. Three weak transitions 526, 593, and 812 keV were observed in coincidence with the 178 and 188 keV gates but could not be placed in the level scheme.

B. Internal conversion electron measurements

Internal conversion electrons (ICE) and γ rays were measured in the reaction ^{40}Ca(^{36}Ar,3p)^{73}Br at 130 MeV. The experiment was performed at the VICKSI accelerator of the Hahn-Meitner Institut, Berlin, using the superconducting electron spectrometer described in detail in Ref. 11. The experimental setup is sketched in Fig. 3. The axis of the superconducting solenoid was perpendicular to the beam which was focused onto a thin target allowing the recoiling nuclei to decay in flight. γ rays were detected in an intrinsic Ge detector of about 25% relative efficiency. The sensitive path length from which electrons were focused onto the 300 mm^2 Si(Li) detector was 20 mm starting at 5 mm downstream from the target. Both detectors were operated in the homogeneous mag-

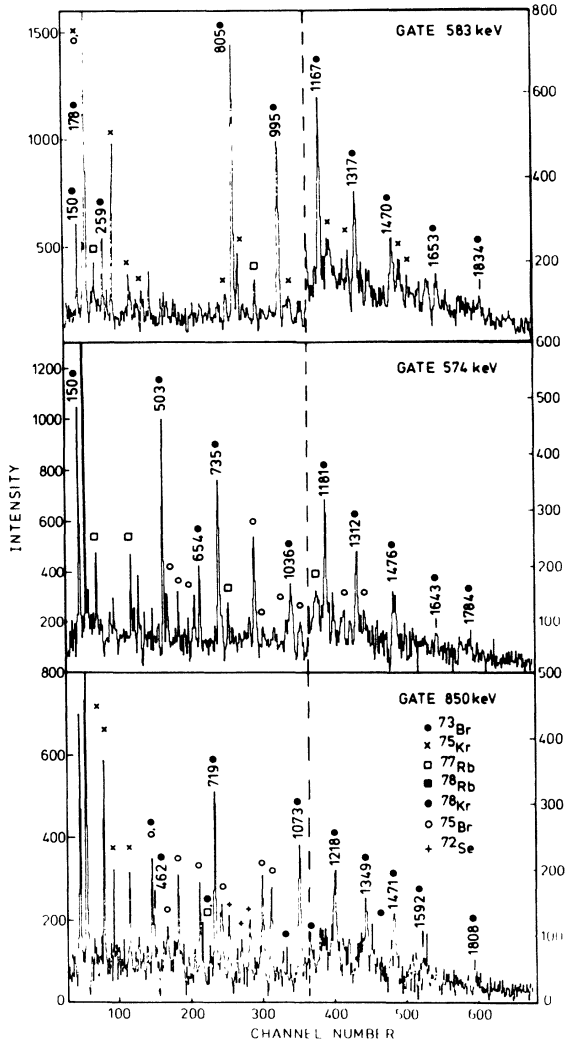

FIG. 1. Coincidence spectra corresponding to the three bands in ^{73}Br measured in the reaction ^{58}Ni(^{24}Mg,2αp)^{73}Br. Known contaminants are marked as shown in the inset.

netic field of 1 T. In addition, a Ge(Li) detector of about 28% relative efficiency was placed at 150° to the beam outside the solenoid.

The target consisted of a 650 μg/cm^2 Ca layer of natural composition sandwiched between a 1.1 mg/cm^2 ^{181}Ta foil and a 4.9 mg/cm^2 ^{209}Bi degrader. The Ca and Bi layers had been evaporated on the Ta substrate foil. ^{181}Ta and ^{209}Bi were chosen in order to avoid long-lived and highly converted transitions from Coulomb excitation producing contaminant conversion electrons. One-third of the recoiling nuclei were stopped in the Bi degrader; the remaining 67% were slowed down to $v/c=0.84(5)$% corresponding to an average recoil velocity $v=0.25$ cm/ns. Due to the shielding of the baffle, only electrons from decays of excited states with lifetimes in the nanosecond range could be detected in the electron detector. The calibration of energies and efficiencies of the 90° gamma and electron detectors was performed *in situ* with a ^{152}Eu source. The relative γ intensities, K and L conversion coefficients, and the K fluorescence yield were taken from Refs. 12–15.

Figure 4 displays a spectrum of the 90° Ge detector gated with electrons. All strong lines originate from γ decays in ^{73}Br and ^{72}Br,[16,17] and from x-ray emission in ^{181}Ta and ^{209}Bi. Figure 5 shows an electron singles spectrum recorded in 9 h. All visible lines are K-conversion lines of ^{73}Br and ^{72}Br transitions. The peak at $E_e=13.3$ keV is the K-conversion peak arising from the decay of the 27 keV state which is directly observed for the first time in the present work. The broad peaks in the spectrum result from kinematic broadening due to the large solid angle $\Omega\approx 2\pi$ covered by the electron detector in a homogeneous magnetic field. The electron peak at $E_e=15.3$ keV is the K-conversion line of the ^{72}Br 30.4 keV transition. However, internal conversion coefficients (ICC) of the ^{72}Br transitions could not be determined due to the unknown lifetimes of the states of interest.

ICC were determined from the γ-ray and K-conversion electron yields at 90°. The angular distributions of γ rays were taken into account using the measured a_2 and a_4 coefficients,[7] but neglected for electrons due to the large coverage of the solid angle. Since the observed γ rays and conversion electrons arise from decays in flight, long-lived states decay in the insensitive part of the spectrometer; therefore, the detection efficiency for long-lived states is reduced. The seven electron lines can be grouped according to their lifetimes and in each group the same efficiency correction factor was used. The transitions of 188, 259, 108, and 46 keV have a lifetime of $\tau=1.6(3)$ ns and the 214 and 63 keV transitions of $\tau=50(2)$ ns. The 178 keV state decays with $\tau=0.69(10)$ ns but is fed via the long-lived 63 and 108 keV transitions.[7] Its correction factor can be calculated from the 286–240 keV cascade. As the absolute detection efficiency could not be determined, the 188 keV line was inferred to be a pure $E2$ transition for reasons discussed below.

The resulting ICC values are listed in Table I and compared in Fig. 6 with the tabulated ICC for dipole and quadrupole transitions.[13] The ICC of the 27 keV line could not be determined due to its unknown lifetime. However, an estimate of the lifetime on the basis of the intensity balance and proposed $E2$ nature (see Sec. III A) yields 1.4 μs $\leq\tau\leq$ 9.1 μs, i.e., only a small fraction of this totally converted line is emitted in the sensitive volume. The error bars of the ICC of the 46 and 63 keV transitions did not allow us to distinguish between $M1$ and $E1$, which differ by only about 20%. Since the $E1$ nature of the 108 keV transition leads to a parity change between the 286 and 178 keV states, one of the cascade transitions must be $E1$ and the other $M1$. The efficiency correction factors for the 63 and 214 keV line are only in agreement if one assumes that they are $M1$ and $E2$ transitions, respectively, leaving an $E1$ character for the 46 keV transition.

III. DISCUSSION

A. Spin and parity assignments

A recent nuclear orientation measurement of the ^{73}Br ground state spin yielded $I=\frac{1}{2}$,[18] in contrast to the previ-

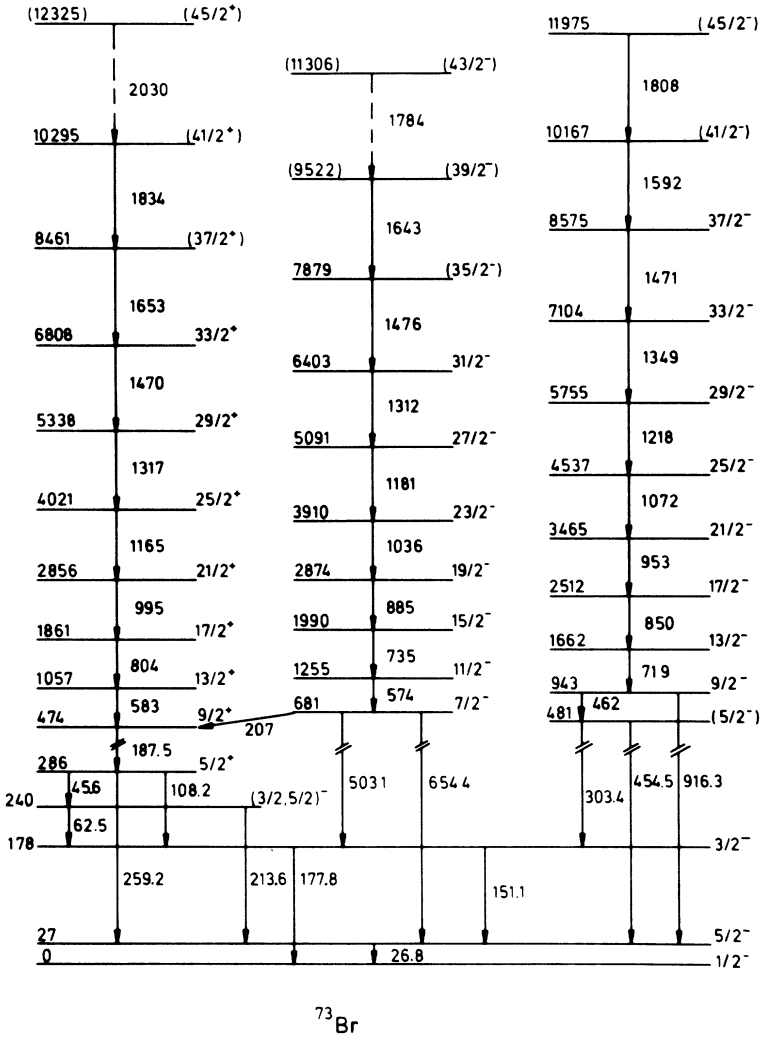

FIG. 2. The newly proposed level scheme of ^{73}Br including the results of Ref. 7.

ously suggested value $I=\frac{3}{2}$. The negative parity of the ground state has been deduced from β-decay work.[19] Since the multipolarity of the 27 keV ground state transition could not be directly measured in the IC experiment, another argument was needed to assign the spins and parities in the ^{73}Br level scheme. Following our previous arguments[7] and the systematics of the energies of the $\frac{9}{2}^+$ states in the odd-A Rb, Br, and As isotopes, the previous assignment $I^\pi(286\text{ keV})=\frac{5}{2}^+$ was kept. The measured angular distribution coefficients and lifetimes[7] support the stretched $E2$ nature of the 187, 583, 995, 1165, 1320, and 1470 keV in-band transitions and thus the spins and parities in the decoupled $g_{9/2}$ band.

The assignment $I^\pi=\frac{3}{2}^-$ for the 178 keV state is uniquely established since the $E2/M1$ 178 keV transition from this state terminates at a $\frac{1}{2}^-$ state. The $E1$ 108 keV transition is consistent with a spin parity of $\frac{5}{2}^+$ for the 286 keV state. The stretched $E2$ nature of the 503 keV transition which is supported by the measured a_2 and a_4 coefficients and the lifetime of the 681 keV state[7] then yields $I^\pi(681\text{ keV})=\frac{7}{2}^-$. The allowed spin differences of the transitions 654 keV ($M1/E2$), 259 keV ($E1$), 151 keV ($M1/E2$),[7] and 214 keV ($E2$) leave only $I^\pi=\frac{5}{2}^-$ for the 27 keV state. Now the stretched $E2$ nature of the 916 keV transition determines $I^\pi(943\text{ keV})=\frac{9}{2}^-$ and the multipolarities of the transitions 46, 63, and 214 keV leave

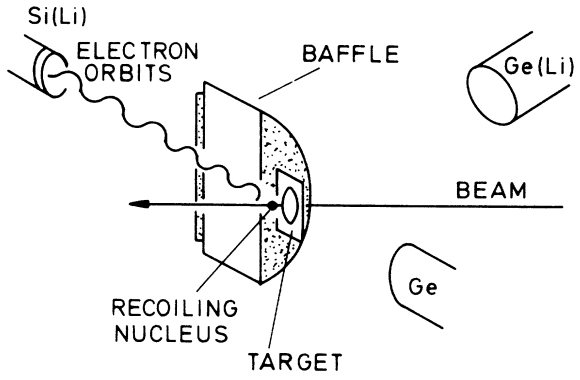

FIG. 3. Sketch of the experimental setup of the conversion electron measurement.

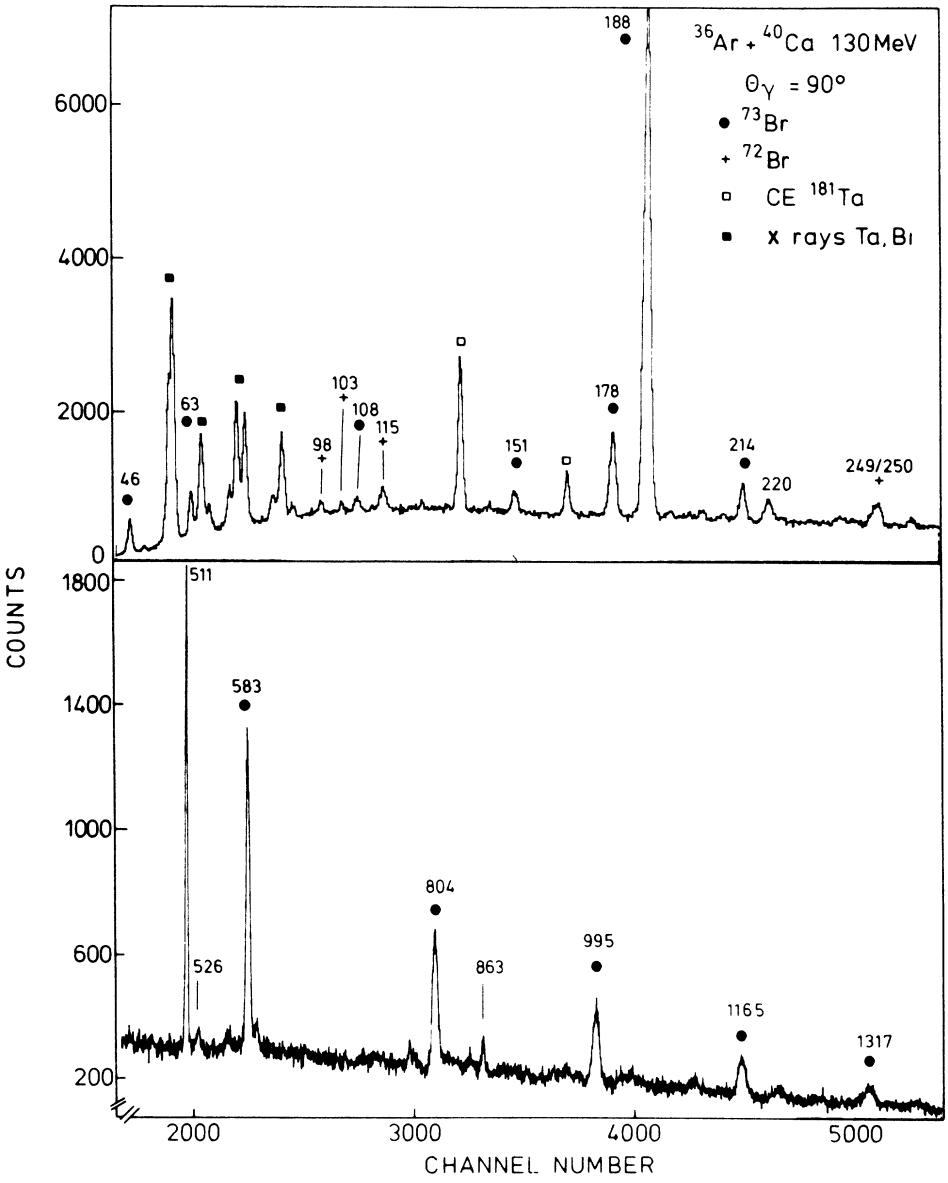

FIG. 4. Spectrum in the 90° Ge detector gated with electrons. The origin of the $e^-\gamma$ coincidences is indicated.

$I^\pi=(\frac{3}{2},\frac{5}{2})^-$ for the 240 keV state. The spin of the 481 keV state could not be determined since the small intensities of the 462, 303, and 455 keV transitions and their expected small ICC values of $\alpha_K \leq 10^{-3}$ did not allow us to measure IC or angular distribution coefficients. However, since the lifetime and the branching ratios of the 943 keV state[7] suggest a stretched $E2$ character of the 462 keV line, the assignment $I^\pi(481\text{ keV})=\frac{5}{2}^-$ is most likely. The spins and parities in the negative-parity bands above 681 keV are determined from the stretched $E2$ nature of the in-band transitions which again follows from the angular distributions and level lifetimes reported in Ref. 7.

B. Shape coexistence and triaxiality in the bandhead region

The measured ^{73}Br ground state spin $I=\frac{1}{2}$ (Ref. 18) deviates from the systematics of the odd-A Br isotopes ^{75,77,79}Br, which all have $I^\pi=\frac{3}{2}^-$. The negative parity of the ^{73}Br ground state follows from the allowed β decay to the 26 keV $\frac{3}{2}^-$ state in ^{73}Se.[19] The large deformation $\beta_2 \approx 0.38$, as deduced from the in-band $E2$ transition strengths,[7] suggests that one would also expect a ground state based on $[312]\frac{3}{2}^-$ Nilsson orbital in ^{73}Br.

The energies of the $1qp$ states have been calculated in

^{75}Br as a function of deformation in an *axially* deformed Woods-Saxon potential using the Strutinsky-Bogolyubov cranking model without pairing.[5] The experimental level order of yrast ($1qp$) bands was reproduced by these calculations. Since ^{73}Br has only two neutrons less than ^{75}Br, one may expect that the calculations used to describe ^{75}Br would require only slight modifications for ^{73}Br, especially if one assumes that most low spin properties are based on the common unpaired proton. This is certainly true for the development of the rotational bands in the two isotopes which are very close in energies and $E2$ transition strengths as pointed out previously.[7] However, the more complex low spin structure of ^{73}Br calls for some caution. A $\frac{1}{2}^-$ state was predicted to be lowest in energy for oblate deformations $-0.05 \geq \beta_2 \geq -0.18$. The experimental level order of the three lowest ^{73}Br states

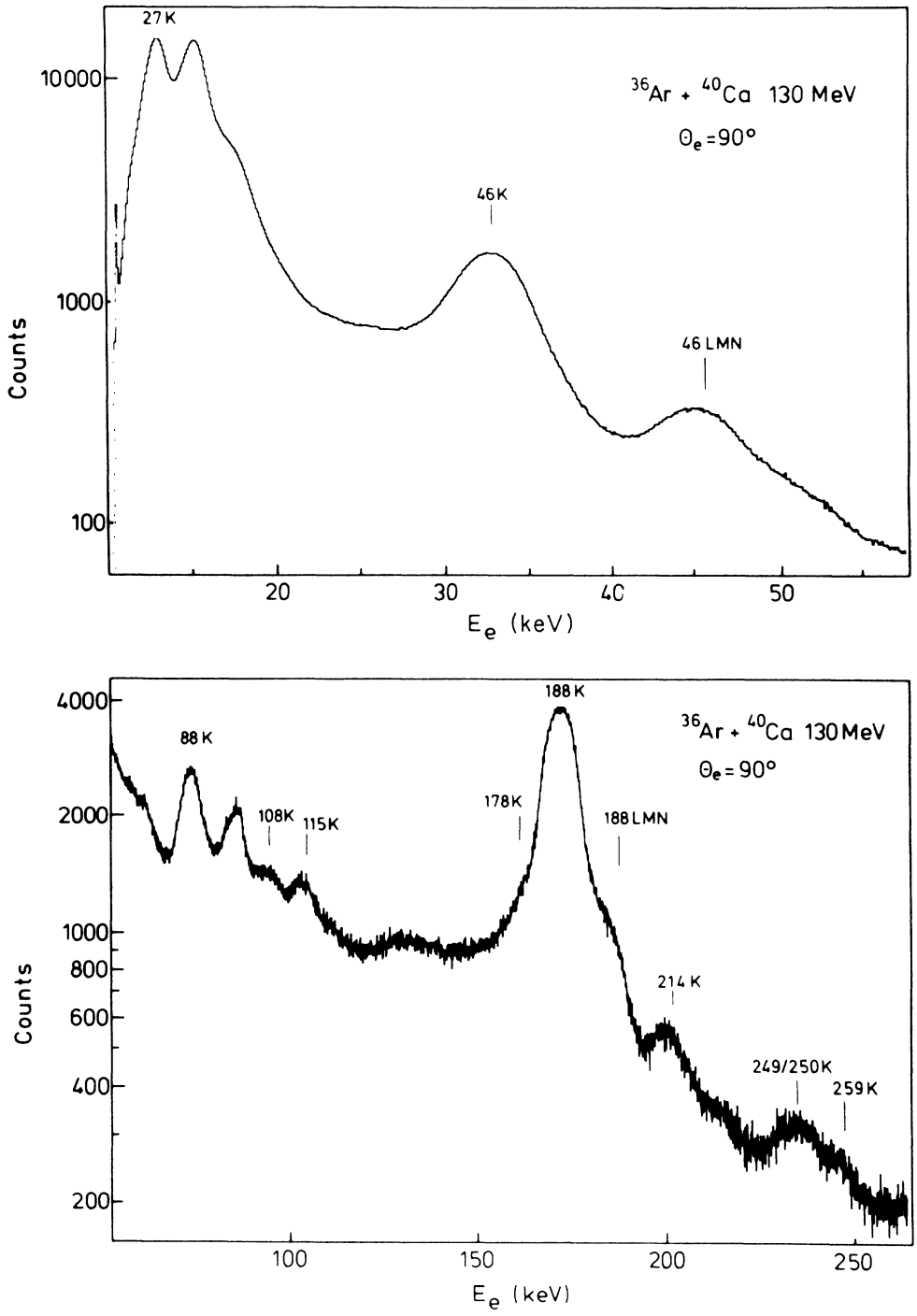

FIG. 5. Singles spectra of conversion electrons recorded in the reaction ^{40}Ca+^{36}Ar at 130 MeV and 90° to the beam.

TABLE I. Relative γ and electron intensities and K-conversion coefficients.

Transition energy (keV)	Electron energy (keV)	I_e[a] (%)	$I_\gamma(90°)$[b] (%)	$I_e/I_\gamma(90°)$[c]	α_K	Multipolarity
27	13.3	42(13)				$E2$[d]
46	32.1	410(29)	36.7(20)	6.3(6)	0.84(8)	$E1$[d]
63	49.0	23.7(17)	13.4(15)	1.00(15)	0.36(6)	$M1$[d]
108	94.7	5.3(4)	6.9(6)	0.382(48)	0.058(7)	$E1$
178	164.3	8.7(6)	53(1)	0.0881(76)	0.031(5)	$M1/E2$[e]
188	174.0	100(2)	100(7)	0.635(46)	0.075(6)	$E2$
214	200.1	4.4(3)	17.6(4)	0.138(12)	0.050(7)	$E2$
259	245.7	1.1(1)	16.5(3)	0.041(3)	0.0050(4)	$E1$

[a]Normalized to the 174 keV line.
[b]Normalized to 188 keV line.
[c]From absolute intensities.
[d]See text.
[e]$|\delta(E2/M1)| = 0.39(12)$.

$(\frac{1}{2}^- \text{-} \frac{5}{2}^- \text{-} \frac{3}{2}^-)$ could not be reproduced by the theory for any deformation parameter. This different level ordering seems difficult to explain in an axially symmetric model without considering shape coexistence.

Many authors pointed out that the transition from prolate to oblate shapes in this mass region rather occurs by a variation of the triaxiality parameter γ. The calculations by Stone *et al.*[18] suggest for a triaxial shape with $\gamma \approx -30°$ a $\frac{1}{2}^-$ ground state with a mixed $[301]\frac{3}{2}^-$-$[321]\frac{1}{2}^-$ structure and a second low-lying negative-parity state. At large prolate deformation, the 178 keV bandhead can most likely be identified with the $[312]\frac{3}{2}^-$ Nilsson orbital. More detailed calculations involving triaxiality have to be carried out to understand the structure of the ^{73}Br bandhead region.

C. Rotational structure and alignment effects

In a recent study of high spin states in ^{75}Br,[8] the rotational structure was established up to probable spin $\frac{45}{2} - \frac{49}{2}$. Band crossings were observed and related to $g_{9/2}$ proton and neutron alignments using blocking arguments and systematics of band crossing frequencies.[10] In the negative-parity yrast bands, the $g_{9/2}$ protons were found to align at a rotational frequency $\hbar\omega \approx 0.38$ MeV, whereas the $g_{9/2}$ neutron alignment takes place at $\hbar\omega = 0.63$–0.65 MeV in both positive- and negative-parity bands. In our previous ^{73}Br study, only one band crossing was observed at $\hbar\omega = 0.43$ MeV in the favored negative-parity band $(\pi = -, \alpha = +\frac{1}{2})$; it was related to $g_{9/2}$ proton alignment.[7] In the present study, the extension of the level

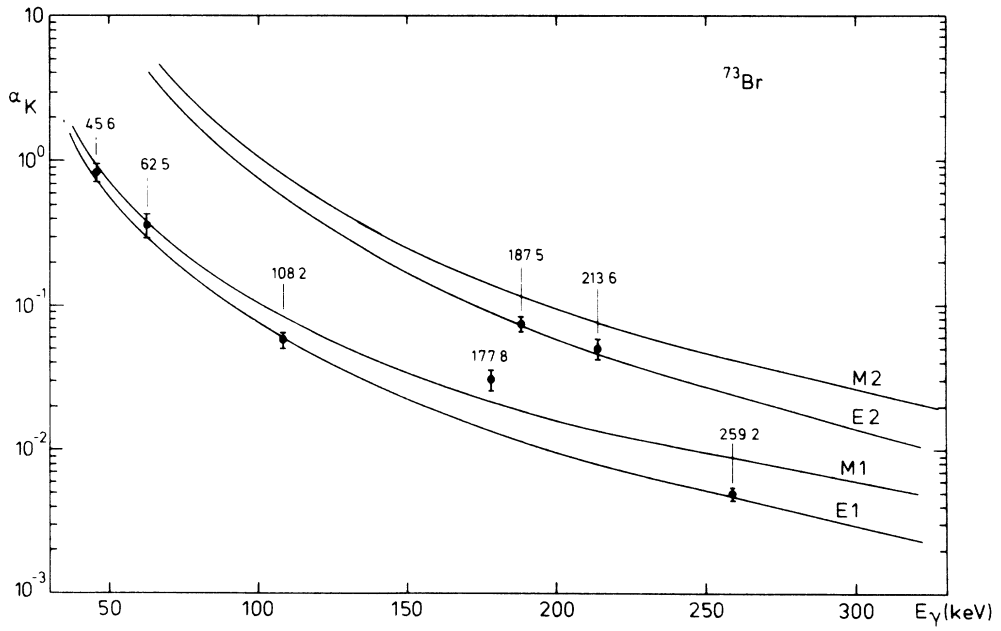

FIG. 6. Comparison of experimental and theoretical conversion coefficients for different multipolarities.

scheme and the comparison with ^{75}Br enabled us to look for neutron alignment effects.

Figure 7 shows the dynamic moments of inertia $J^{(2)}$ as a function of the rotational frequency $\hbar\omega$ for the positive- and negative-parity bands in ^{73}Br and ^{75}Br. The $J^{(2)}$ moments were calculated using a projection $\Omega=\frac{3}{2}$ of the single-particle angular momentum on the symmetry axis for both parities. We note the following features: (1) The variations of $J^{(2)}$ in ^{73}Br are much weaker than in ^{75}Br; the maxima of $J^{(2)}$ are barely visible. (2) The $g_{9/2}$ neutron alignment in the positive-parity band is found in the same frequency interval $\hbar\omega=0.6$–0.7 MeV in both isotopes. (3) In the negative-parity states, the $g_{9/2}$ protons in the $\alpha=+\frac{1}{2}$ band and the $g_{9/2}$ neutrons in the $\alpha=-\frac{1}{2}$ band seem to align simultaneously in ^{73}Br and ^{75}Br at $\hbar\omega=0.42$ MeV and $\hbar\omega=0.60$ MeV, respectively. (4) The neutron alignment in the $(\pi=-,\alpha=+\frac{1}{2})$ band appears as a broad peak at $\hbar\omega=0.65$–0.80 MeV. (5) The proton alignment in the $(\pi=-,\alpha=-\frac{1}{2})$ band, which is also expected to take place at $\hbar\omega\approx0.40$ MeV, can barely be seen.

The damping of the $J^{(2)}$ peaks in ^{73}Br compared to ^{75}Br suggests that the interaction between the 1(3)*qp* and 3(5)*qp* bands increases when going from $N=40$ to $N=38$. The weak alignment effects can be related to the gap in the single-particle energies for $Z,N=38$ at large prolate deformations. Nazarewicz and Werner[20] showed that the occupation of orbitals right below the gap leads to a reduction of the gap parameter Δ and thus near-rigid rotation, as discussed in more detail for ^{77}Rb (Ref. 21) and ^{76,78}Kr.[10] The previously reported reductions of the transitional quadrupole moments in the bands of ^{73,75}Br (Refs. 5 and 7) starting at $\hbar\omega\geq0.4$ MeV may be related to the $g_{9/2}$ neutron crossing.

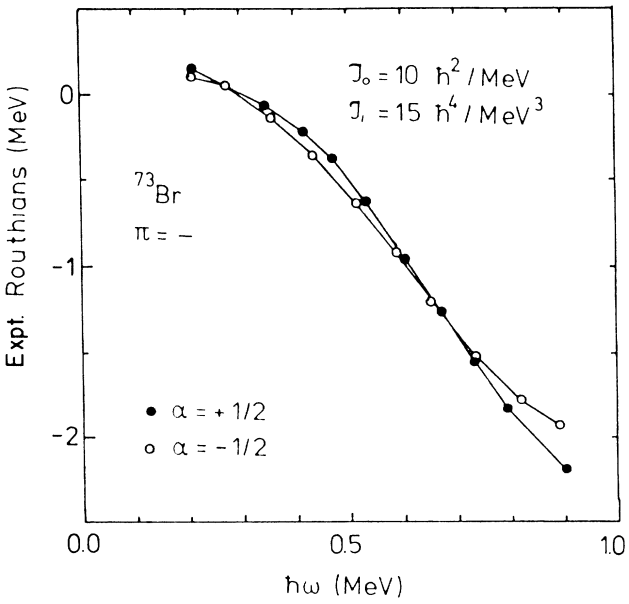

FIG. 8. Experimental negative-parity Routhians in ^{73}Br.

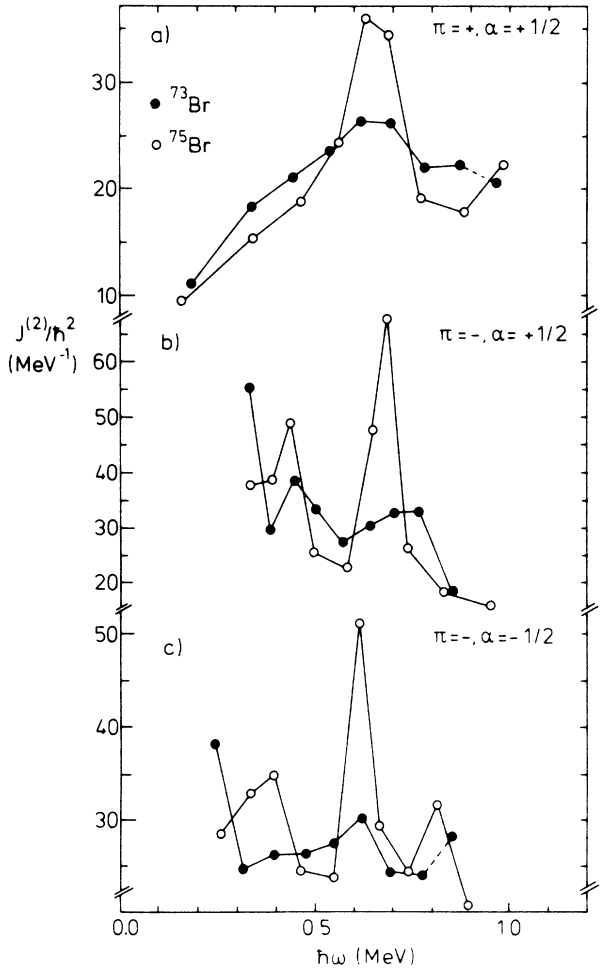

FIG. 7. Dynamic moments of inertia $J^{(2)}$ as a function of the rotational frequency $\hbar\omega$ for the bands in ^{73}Br and ^{75}Br (Ref. 8).

Effects of triaxiality in the higher members of the bands have not been discussed so far. Experimental evidence for triaxial shapes can be obtained from the signature dependence of the $E2$ or $M1$ strengths of the $\Delta I=1$ $\alpha=+\frac{1}{2}\rightarrow\alpha=-\frac{1}{2}$ transitions or from the signature inversion of the Routhians.[22] However, since no $(\pi=+,\alpha=-\frac{1}{2})$ band and no $\Delta I=1$ transitions in the negative-parity bands have been observed, only little experimental information about triaxiality is available. One hint for triaxial shapes in the negative-parity states is presented in Fig. 8, which shows the experimental negative-parity Routhians. The Harris parameters are inserted and have been chosen similar to ^{75}Br.[5] In the frequency range $\hbar\omega=0.30$–0.65 MeV, the $\alpha=-\frac{1}{2}$ Routhian is below the $\alpha=+\frac{1}{2}$ Routhian. This signature inversion may, similar to ^{75}Br, be related to a change in deformation from $\gamma<0$ to $\gamma>0$.

D. The ^{73}Kr ground state

The new spin-parity assignments in ^{73}Br allow us to deduce the so far unknown spin and parity of the ^{73}Kr

TABLE II. Newly calculated log(ft) values for the β decay of ^{73}Kr assuming either a 10% branch (A) or a 50% branch (B) of the β-decay intensity feeding the 27 keV and ground state.

Level energy (keV)	Spin I	A $I_{\beta+}$[a] (%)	A log(ft)	B $I_{\beta+}$[a] (%)	B log(ft)
681	$\frac{7}{2}^-$	8.3	6.1	4.6	6.4
481	$(\frac{5}{2}^-)$	13.5	5.9	7.5	6.1
473		7.4	6.1	4.1	6.4
392		4.8	6.3	2.7	6.6
329		3.0	6.5	1.7	6.8
241	$(\frac{3}{2},\frac{5}{2})^-$	17.8	5.8	9.9	6.0
178	$\frac{3}{2}^-$	35.2	5.5	19.6	5.7
27	$\frac{5}{2}^-$	10.0[b]	6.0	50.0[b]	5.3
0	$\frac{1}{2}^-$				

[a]Normalized recalculated intensities based on the average intensities from Davids and Goosman (Ref. 24) and Roeckl *et al.* (Ref. 25).
[b]Assumed branch.

ground state that has an adopted half-life of 27.0(12) s.[23] A recent compilation of $A=73$ data[23] showed that the log(ft) values for the decay of the ^{73}Kr ground state to the 681 keV $\frac{7}{2}^-$ and the 178 keV $\frac{3}{2}^-$ state in ^{73}Br are allowed transitions with log(ft)=5.9 and log(ft)=5.8, respectively. In the previous β-decay studies of ^{73}Kr,[24–26] only γ-ray energies and intensities were measured. However, since in the previous work the 654 keV line and the 27 keV converted transition were not observed and the transitions of 151, 214, and 303 keV were not placed correctly in the ^{73}Br level scheme, we recalculated the log(ft) values with the new levels and branching ratios. Table II lists the log(ft) values assuming either a total 10% branch (A) or a 50% branch (B) of the total β-decay intensity to feed the 27 keV and the ground state. The log(ft) values for the decays to the 681, 481, 241, and 178 keV states are in all cases within the limits for allowed transitions, leaving a ^{73}Kr ground state spin and parity of $I^\pi=\frac{5}{2}^-$. Davids and Goosman[24] had ruled out a strong nonobserved branch to the ^{73}Br ground state on the basis of ^{73}Br buildup and decay. A missing intensity of 10–20% (to the ground and 27 keV states) is possible within their errors and would be compatible with an allowed decay to the 27 keV $\frac{5}{2}^-$ level. Therefore, the $\frac{5}{2}^-$ spin-parity assignment to the ^{73}Kr ground state is not in conflict with any experimental data. In a test experiment, a recoil catcher was inserted in the electron spectrometer and low energy conversion electrons were looked for off beam. However, the low ^{73}Kr population cross section and the small electron energy did not allow us to observe this branch.

IV. CONCLUSIONS

In the present study, conversion coefficients of seven low energy transitions in the bandhead region of ^{73}Br have been measured. These, together with the newly determined ground state spin parity of $\frac{1}{2}^-$,[18] have allowed us to establish new spin-parity assignments. The level order of the low-lying states suggests shape coexistence effects as found in the neighboring light Se isotopes $^{69-72}$Se. However, the occurrence of several $\frac{3}{2}^-$ and $\frac{5}{2}^-$ states below 500 keV excitation energy is not yet completely explained. Triaxial shapes in the observed bands cannot be ruled out. In all bands, broad peaks in the dynamic moments of inertia versus angular frequency plots are observed at rotational frequencies $\hbar\omega=0.6$–0.8 MeV. In analogy with similar effects in ^{75}Br, these peaks are associated with $g_{9/2}$ neutron alignment. The weak alignment effects in ^{73}Br as compared to ^{75}Br imply that the band interactions in ^{73}Br are larger than in ^{75}Br. From the allowed log(ft) values for the decays to the ^{73}Br $\frac{7}{2}^-$ and $\frac{3}{2}^-$ states, the ^{73}Kr ground state is suggested to have $I^\pi=\frac{5}{2}^-$.

ACKNOWLEDGMENTS

The authors would like to thank C. J. Lister, W. Gelletly, B. J. Varley, A. A. Chishti, and J. H. McNeill for their assistance in the $\gamma\gamma$ experiment. We thank the tandem crew at Daresbury and the VICKSI operators at Berlin for providing excellent beams. This work was supported by the German Bundesministerium für Forschung und Technologie (BMFT) under Contract No. 06Gö141.

*Permanent address: Institute of Modern Physics, Academia Sinica, Lanzhou, People's Republic of China.

[1]J. Heese, K. P. Lieb, L. Lühmann, F. Raether, B. Wörmann, D. Alber, H. Grawe, J. Eberth, and T. Mylaeus, Z. Phys. A **325**, 45 (1986).

[2]J. H. Hamilton, A. V. Ramayya, W. T. Pinkston, R. M. Ronningen, G. Garica-Bermudez, H. K. Carter, R. L. Robinson, H. J. Kim, and R. O. Sayer, Phys. Rev. Lett. **32**, 239 (1974).

[3]K. P. Lieb and J. J. Kolata, Phys. Rev. C **15**, 939 (1977).

[4]T. Mylaeus and J. Eberth, private communication.

[5]L. Lühmann, M. Debray, K. P. Lieb, W. Nazarewicz, B. Wörmann, J. Eberth, and T. Heck, Phys. Rev. C **31**, 828 (1985).

[6]B. Wörmann, J. Heese, K. P. Lieb, L. Lühmann, F. Raether, D. Alber, H. Grawe, and B. Spellmeyer, Z. Phys. A **322**, 171 (1985).

[7]J. Heese, K. P. Lieb, L. Lühmann, S. Ulbig, B. Wörmann, D. Alber, H. Grawe, H. Haas, and B. Spellmeyer, Phys. Rev. C **36**, 2409 (1987).

[8]N. Martin, C. J. Gross, J. Heese, and K. P. Lieb, J. Phys. G **15**, L123 (1989).

[9]C. J. Gross, J. Heese, K. P. Lieb, C. J. Lister, B. J. Varley, A. A. Chishti, J. H. McNeill, and W. Gelletly, Phys. Rev. C **39**, 1780 (1989).

[10]C. J. Gross, J. Heese, K. P. Lieb, S. Ulbig, W. Nazarewicz, C. J. Lister, B. J. Varley, J. Billowes, A. A. Chishti, J. H. McNeill, and W. Gelletly, Nucl. Phys. **A501**, 367 (1989).

[11]M. Guttormsen, A. v. Grumbkov, Y. K. Argawal, K. P. Blume, K. Hardt, H. Hübel, J. Recht, P. Schüler, H. Kluge, K. H. Maier, A. Maj, and N. Roy, Nucl. Phys. **A398**, 119 (1983).

[12]D. Mehta, M. L. Garg, J. Singh, N. Singh, T. S. Cheema, and P. N. Trehan, Nucl. Instrum. Methods **245A**, 447 (1986).

[13]F. Rösel, H. M. Fries, K. Alder, and H. C. Pauli, At. Data Nucl. Data Tables **21**, 291 (1978).

[14]W. Bambynek, B. Crasemann, R. W. Fink, H.-U. Freund, H. Mark, C. D. Swift, R. E. Price, and P. Venugopala Rao, Rev. Mod. Phys. **44**, 716 (1972).

[15]V. A. Sergienko, A. V. Vorontsovski, and M. A. Naim, Izv. Akad. Nauk SSSR, Ser. Fiz. **49**, 891 (1985).

[16]G. Garcia-Bermudez, C. Baktash, A. J. Kreiner, and M. A. J. Mariscotti, Phys. Rev. C **25**, 1396 (1982).

[17]S. Ulbig, F. Cristancho, J. Heese, K. P. Lieb, T. Osipowicz, B. Wörmann, J. Eberth, T. Mylaeus, and M. Wiosna, Z. Phys. A **329**, 51 (1988).

[18]N. J. Stone, C. J. Ashworth, I. S. Grant, A. G. Griffiths, S. Ohya, J. Rikovska, and P. M. Walker, in *Nuclear Structure of the Zirconium Region,* edited by J. Eberth, R. A. Meyer, and K. Sistemich (Springer, Berlin, 1988), p. 309.

[19]G. Murray, W. J. K. White, J. C. Willmott, and R. F. Entwistle, Nucl. Phys. **A142**, 21 (1970).

[20]W. Nazarewicz and T. Werner, in *Nuclear Strucuture of the Zirconium Region,* edited by J. Eberth, R. A. Meyer, and K. Sistemich (Springer, Berlin, 1988), p. 277.

[21]L. Lühmann, K. P. Lieb, C. J. Lister, B. J. Varley, J. W. Olness, and H. G. Price, Europhys. Lett. **1**, 623 (1986).

[22]I. Hamamoto (unpublished).

[23]M. M. King, Nucl. Data Sheets **51**, 161 (1987).

[24]C. N. Davids and D. R. Goosman, Phys. Rev. C **8**, 1029 (1973).

[25]E. Roeckl, D. Lode, K. Böckmann, B. Neidhart, G. K. Wolf, W. Lauppe, V. Kaffrell, and P. Patzelt, Z. Phys. **266**, 65 (1974).

[26]H. Schmeing, J. C. Hardy, R. L. Graham, J. S. Geiger, and K. P. Jackson, Phys. Lett. **44B**, 449 (1973).